How could 50°C be reached in Paris: analysing the CMIP6 ensemble to design storylines for adaptation

Pascal Yiou, Robert Vautard, Yoann Robin, Nathalie N. de Noblet-Ducoudré, Fabio d'Andrea, Robin Noyelle

How could 50°C be reached in Paris: analysing the CMIP6 ensemble to design storylines for adaptation

Pascal Yiou (1), Robert Vautard (1), Yoann Robin (1), Nathalie de Noblet-Ducoudré (1), Fabio D'Andrea (2), Robin Noyelle (1)

(1) Laboratoire des Sciences du Climat et de l'Environnement, UMR8212 CEA-CNRS-UVSQ, IPSL & Université Paris-Saclay, 91191 Gif-sur-Yvette, France
(2) Laboratoire de Météorologie Dynamique, UMR CNRS-X-ENS, IPSL & Université PSL, 75005 Paris, France

Keywords
Heatwaves, CMIP6, Model selection, Paris

Abstract
Reaching a surface temperature of 50°C in a heavily populated region, like Paris, would have devastating effects. Although such a high value seems far from the present-day record of 42.6°C, its occurrence cannot be dismissed by the end of the 21st century, due to the continuous increase of global mean temperature. In this paper, we address two questions that were asked by the City of Paris to a group of scientists: When does this event start to be likely? What are the prevailing meteorological conditions? We base our study on the CMIP6 simulation ensemble. Many of the CMIP6 yield biases in temperature. Rather than using methods of bias correction, which are not necessarily adapted to high extremes, we propose a pragmatic approach of model selection in order to seek such high temperature events that are deemed realistic. We analyze the meteorological conditions leading to first occurrences of such hot events and their common atmospheric patterns. This paper describes a simple data mining approach (on a large ensemble of climate model simulations) which could be adapted to other regions of the world, in order to help decision makers anticipating and adapting to such devastating meteorological events.

1 Introduction
Heatwaves have huge impacts on society and ecosystems (Domeisen et al., 2023; Bastos et al., 2020; Yin et al., 2023), and frequently generate thousands of extra deaths per summer in Europe. Western European governments took measures to lower vulnerability, after the European heatwaves in 2003. The Pacific North West American heat wave in June 2021 was a

shock with temperatures that came close to 50°C during a couple of days, and were way above previous historical records (Philip et al., 2022). The authorities of a few major cities (in particular in Europe) are in the process of designing adaptation plans to such events, yet unprecedented in Europe, where records since 1950 reach 40-45°C, except for a few Mediterranean cities (Athens, Syracuse, Cordoba), with record nearing or exceeding 48°C. The city of Paris, with a record (2019) of 42.6°C, s preparing an adaptation plan to extreme summer temperatures, and a crisis plan for temperatures in the range of 50°C (Florentin and Lelievre, 2023). Scientific questions that have been asked to the (French) scientific community are:

1. Can temperatures exceed 50°C in Paris and for how long?
2. What is a likely horizon for the first occurrence of such an event?
3. How are the 50°C reached?

The record shattering event across Western Canada and the US in 2021 (i.e., at a similar latitude as the Paris area) suggests that one could not dismiss that such a hot event could occur in Europe in years/decades to come. Such temperatures were also observed in southern Europe in 2021 and 2023. Therefore, preparing a crisis exercise and adaptation plans for that level of temperatures is important now, as adaptation actions will take time to be effective.
When daily temperature records are broken, the increments above the previous record are generally a few tenths of degrees. In the Pacific NorthWest American event in summer in 2021, this was called a “record shattering” event because records were broken by several degrees (Fischer et al., 2021). Such record shattering events can be seen as outliers of observed extreme value distributions (Fischer et al., 2023), and hence can be qualified as surprises. Using data from 1950, Philip et al. (2022) estimated a return period for the event of the order of about 1000 year, accounting for the current global warming level. (Bador et al., 2017) have investigated temperature records in regional climate projections. Based on a single climate model, they found the possibility to exceed locally 50°C in France but not in the Paris region. Here we are interested in hot events that would occur as surprises, similarly to the recent events of 2021 or 2023. Such events are deemed to have a low probability (Philip et al., 2022), which requires large ensemble of data (Bevacqua et al., 2023).

The objective of this article is to present a method that allows analyzing the possibility of temperatures to reach 50°C in the Paris and provide physically plausible example cases which can serve city managers and planners for adaptation reference using recent climate projections. The recent CMIP6 simulations offer a large multi-model ensemble of data, with several socio-economic scenarios until the end of the 21st century.
This paper also aims at succinctly describing the conditions under which temperatures of 50°C can be reached in a highly populated European region like Ile-de-France, surrounding Paris (France). We examine the large-scale atmospheric conditions for such an event, and the global warming level above which such conditions are found with significant probabilities in the simulations, accounting for the interannual and interdecadal variability. We mainly describe a data processing chain, and defer a complete physical analysis to another paper.

This description can lead to a *climate service*, to analyze a large ensemble of climate simulations, and provide sensible answers to the challenges outlined in this introduction (Is it possible to reach 50°C? When? What climatic and meteorological conditions to expect?). The goal is to be able to replicate our analyses easily and change parameters, so that the computations can be transposed to other regions of the planet. Although those data are publicly available, their volume is huge (peta-bytes of data). Treating an ensemble such as

CMIP6 requires scientific computer skills and R&D resources, which are rarely available from city practitioners whose main interest is not atmospheric sciences. It is hence deemed useful to propose a simple methodology, easily reproducible by companies providing consulting or climate services, to treat the three challenges outlined above from available data. Hence, this processing chain is intended for entities that are capable of processing climate model data, and communicate results to final stakeholders. To potentially become useful for other cities, such a methodology should be easy to deploy, reproducible and testable on many regions. We however restrict here to the Paris city for the presentation.

Section 2 presents data and models used in this paper. Section 3 presents results on the occurrence of events that reach 50°C in the Paris area. Section 4 discusses the caveats of the analyses. Section 5 the practical applications of this paper, which is concluded in Section 6.

2 Data and methods

2.1 Data

This analysis uses observations (Haylock et al., 2008), reanalyses (Hersbach et al., 2020) and CMIP6 simulations (Eyring et al., 2016). The CMIP6 simulations include "historical" and four Shared Socioeconomic Pathway (SSP) scenarios (Riahi et al., 2017): 1-2.6, 2-4.5, 3-7.0 and 5.8.5. Historical simulations run from 1860 to 2014, and are constrained by observed forcings (natural and anthropogenic). SSP simulations go from 2015 to 2100 (2300 for some models) and are constrained by economic scenarios of greenhouse gas emissions, pollutants and changes in land use.

Some models provide ensembles of simulations, with slightly perturbed initial conditions. This helps assessing the role of internal climate variability (Deser et al., 2016).

Overall, we considered all simulations that were available to us on August 1st 2023 on the IPSL computing server, which contains a (large) subset of the simulations on the Earth System Grid Federation (ESGF) that contains all CMIP6 simulations. We used the models for which historical runs and the four SSP scenarios are available. This includes 1288 simulations from 26 climate models. Hence this excludes models with fewer scenario simulations. The ensemble sizes for each model (with historical and four SSP scenario simulations) are indicated in Table 1 below. The ensemble sizes vary from 1 run to more than 50 in SSP simulations, depending on the model. The size of the ensembles also depends on the SSP scenarios.

Model	Scenario	Ensemble size	Model	Scenario	Ensemble size
ACCESS-CM2	historical	10	GFDL-ESM4	historical	3
ACCESS-CM2	ssp126	3	GFDL-ESM4	ssp126	1
ACCESS-CM2	ssp245	3	GFDL-ESM4	ssp245	1
ACCESS-CM2	ssp370	3	GFDL-ESM4	ssp370	1
ACCESS-CM2	ssp585	5	GFDL-ESM4	ssp585	1
ACCESS-ESM1-5	historical	40	INM-CM4-8	historical	1
ACCESS-ESM1-5	ssp126	10	INM-CM4-8	ssp126	1
ACCESS-ESM1-5	ssp245	18	INM-CM4-8	ssp245	1
ACCESS-ESM1-5	ssp370	10	INM-CM4-8	ssp370	1
ACCESS-ESM1-5	ssp585	40	INM-CM4-8	ssp585	1
AWI-CM-1-1-MR	historical	5	INM-CM5-0	historical	10
AWI-CM-1-1-MR	ssp126	1	INM-CM5-0	ssp126	1
AWI-CM-1-1-MR	ssp245	1	INM-CM5-0	ssp245	1

AWI-CM-1-1-MR	ssp370	5	INM-CM5-0	ssp370	5
AWI-CM-1-1-MR	ssp585	1	INM-CM5-0	ssp585	1
BCC-CSM2-MR	historical	3	**IPSL-CM6A-LR**	historical	33
BCC-CSM2-MR	ssp126	1	**IPSL-CM6A-LR**	ssp126	6
BCC-CSM2-MR	ssp245	1	**IPSL-CM6A-LR**	ssp245	11
BCC-CSM2-MR	ssp370	1	**IPSL-CM6A-LR**	ssp370	11
BCC-CSM2-MR	ssp585	1	**IPSL-CM6A-LR**	ssp585	7
CAMS-CSM1-0	historical	1	KACE-1-0-G	historical	3
CAMS-CSM1-0	ssp126	1	KACE-1-0-G	ssp126	3
CAMS-CSM1-0	ssp245	1	KACE-1-0-G	ssp245	3
CAMS-CSM1-0	ssp370	1	KACE-1-0-G	ssp370	3
CAMS-CSM1-0	ssp585	1	KACE-1-0-G	ssp585	3
CanESM5	historical	50	**MIROC-ES2L**	historical	31
CanESM5	ssp126	50	**MIROC-ES2L**	ssp126	3
CanESM5	ssp245	50	**MIROC-ES2L**	ssp245	30
CanESM5	ssp370	50	**MIROC-ES2L**	ssp370	1
CanESM5	ssp585	50	**MIROC-ES2L**	ssp585	2
CMCC-ESM2	historical	1	MIROC6	historical	50
CMCC-ESM2	ssp126	1	MIROC6	ssp126	50
CMCC-ESM2	ssp245	1	MIROC6	ssp245	50
CMCC-ESM2	ssp370	1	MIROC6	ssp370	3
CMCC-ESM2	ssp585	1	MIROC6	ssp585	50
CNRM-CM6-1	historical	30	**MPI-ESM1-2-HR**	historical	10
CNRM-CM6-1	ssp126	1	**MPI-ESM1-2-HR**	ssp126	2
CNRM-CM6-1	ssp245	1	**MPI-ESM1-2-HR**	ssp245	2
CNRM-CM6-1	ssp370	3	**MPI-ESM1-2-HR**	ssp370	10
CNRM-CM6-1	ssp585	1	**MPI-ESM1-2-HR**	ssp585	2
CNRM-ESM2-1	historical	10	MPI-ESM1-2-LR	historical	31
CNRM-ESM2-1	ssp126	1	MPI-ESM1-2-LR	ssp126	10
CNRM-ESM2-1	ssp245	1	MPI-ESM1-2-LR	ssp245	10
CNRM-ESM2-1	ssp370	3	MPI-ESM1-2-LR	ssp370	10
CNRM-ESM2-1	ssp585	1	MPI-ESM1-2-LR	ssp585	30
EC-Earth3	historical	73	**MRI-ESM2-0**	historical	12
EC-Earth3	ssp126	2	**MRI-ESM2-0**	ssp126	1
EC-Earth3	ssp245	30	**MRI-ESM2-0**	ssp245	9
EC-Earth3	ssp370	52	**MRI-ESM2-0**	ssp370	5
EC-Earth3	ssp585	58	**MRI-ESM2-0**	ssp585	5
EC-Earth3-Veg	historical	9	NorESM2-LM	historical	3
EC-Earth3-Veg	ssp126	5	NorESM2-LM	ssp126	1
EC-Earth3-Veg	ssp245	6	NorESM2-LM	ssp245	3
EC-Earth3-Veg	ssp370	4	NorESM2-LM	ssp370	3
EC-Earth3-Veg	ssp585	8	NorESM2-LM	ssp585	1
EC-Earth3-Veg-LR	historical	3	**NorESM2-MM**	historical	3
EC-Earth3-Veg-LR	ssp126	3	**NorESM2-MM**	ssp126	1
EC-Earth3-Veg-LR	ssp245	3	**NorESM2-MM**	ssp245	2
EC-Earth3-Veg-LR	ssp370	3	**NorESM2-MM**	ssp370	1

EC-Earth3-Veg-LR	ssp585	3	**NorESM2-MM**	ssp585	1
FGOALS-g3	historical	5	TaiESM1	historical	1
FGOALS-g3	ssp126	4	TaiESM1	ssp126	1
FGOALS-g3	ssp245	4	TaiESM1	ssp245	1
FGOALS-g3	ssp370	5	TaiESM1	ssp370	1
FGOALS-g3	ssp585	4	TaiESM1	ssp585	1

Table 1: List of CMIP6 models and ensemble sizes for each scenario that are treated in this paper. We only indicate the models for which historical and four SSP scenario runs are available. We excluded the models based on MOHC, as they yield documented anomalous behavior for TX. The models in boldface characters are those which pass the Kolmogorov-Smirnov test of a comparison with ERA5 and E-OBS data.

We considered TX (daily maximum temperature), TG (daily mean temperature) and TN (daily minimum temperature) over France, and SLP (sea-level temperature) over the North Atlantic region, in order to investigate the synoptic conditions during heat events in Paris.
In the selection of models, we removed simulations of the HadGEM3-GC31-HH, HadGEM3-GC31-HM, HadGEM3-GC31-LL, HadGEM3-GC31-LM, HadGEM3-GC31-MH, HadGEM3-GC31-MM, and UKESM1-0-LL models. For those models, the errata documentation for CMIP6 states that: "An issue has been discovered where isolated and irregular events are leading to spikes (a single time step) in the value of surface air temperature lead to the value of daily tasmax [1]datasets in all MOHC simulations that include the atmosphere. Initial investigations on a single simulation suggest that events over 340K occur once in every 250 days, with events above 350K occurring once in every 1,200 days. We believe the spikes in tasmax are triggered by the model's surface energy balance, at isolated grid cells, being dominated by sensible heating. For very short periods the accumulated heat appears not to be efficiently mixed away from the surface by the model's sub-grid scale mixing scheme resulting in the spurious values […]". (https://errata.ipsl.fr/static/view.html?uid=76b3f818-d65f-c76b-bfd8-cae5bc27825c).

We extracted TX, TN and TG over the Paris region (Ile de France) outlined in Figure 1. A bilinear interpolation was performed on the model grid cells over the [1.75-3.25°E; 48.25-49.25°N] region, which includes the administrative area of the City of Paris. This interpolation procedure is necessary because Ile de France can be across several model gridcells, whose size can be much larger (~2°) than the area of the region itself. When the spatial average across the region is computed, this interpolation allows weighting the model grid cell that cover the Ile de France region. We note that this computation takes ~28h (for each variable) on the IPSL computing cluster, using 8 parallel CPUs.

We computed the yearly global mean surface temperature (GMST) for each CMIP6 model. The GMST value between 1950 and 2000 is around ~14.1 +/- 0.5°C (1 sigma) for the CMIP6 historical simulations. The mean GMST in ERA5 for these decades is ~13.5°C. We determine global warming increase (GWI) as the difference of a 20-year average GMST with the average value at the turn of the 21st century (1950-2000) or at the turn of the 20th century (1850-1900). A generic code for extracting time series over a given region from the whole CMIP6 archive is provided on github [https://github.com/pascalyiou/Paris50C.git].

[1] Tasmax is equivalent to TX. The citation is reproduced verbatim.

We also used TG from the ERA5 reanalysis (Hersbach et al., 2020) and EOBS (Haylock et al., 2008) data as references to select CMIP6 data (the selection procedure is detailed below). We downloaded the data for the Paris area from the Climate Explorer (https://www.climexp.knmi.nl).

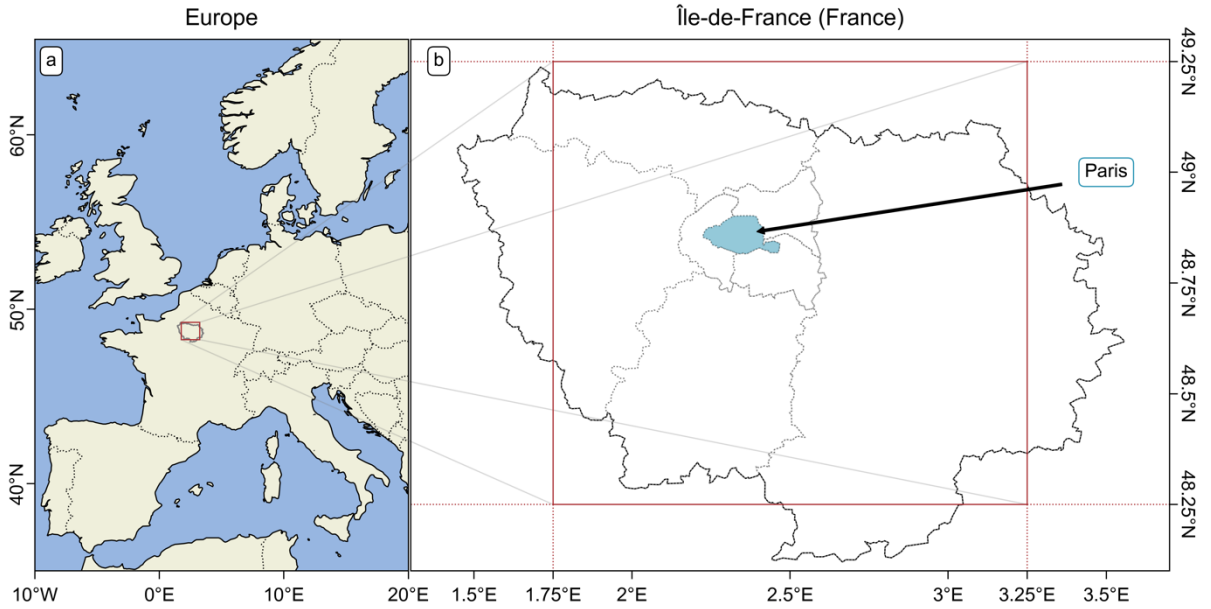

Figure 1: Ile de France Area in Western Europe (panel a). The red rectangle in panel b refers to the region that is considered in the model and reanalysis data. Paris "intra-muros" is indicated in blue.

2.2 Pre-processing

All CMIP6 models are prone to biases, in particular due to their horizontal resolution (Carvalho et al., 2021). One way to solve this issue is to use bias correction methods (Maraun and Widmann, 2018). Such an approach requires a "sound" reference, like a very high-resolution reanalysis (e.g., SAFRAN (Quintana-Segui et al., 2008)), which is not necessarily available everywhere in the world. In addition, such bias correction methods are rather computer costly, and have only been performed on a small subset of CMIP6 (e.g., only one member per model/group, for arbitrarily selected models). Finally, the bias correction of each individual simulation crunches model statistics towards the statistics of one realization of the true climate variability over a limited time period (the correction training period), the observed one, and may thus artificially reduce the simulated natural variability. This effect can be particularly exacerbated for extremes, because the interdecadal variability at regional scale can be large.

We chose here an alternative approach consisting of selecting models yielding the smallest biases over Ile de France of the "historical" simulation for TG, taking advantage of the large number of simulations available in CMIP6. We made a comparison of TG in historical CMIP6 model simulations with ERA5 and EOBS between 1995 and 2014. We performed a Kolmogorov-Smirnov (k-s) test (von Storch and Zwiers, 2001) between each historical simulation, and ERA5 (and EOBS), to compare the probability distributions of daily summer TG in CMIP6 models and reanalyses or EOBS. The threshold we consider for the k-s test value is 0.1. We opted for an "inclusive" approach for model selection: the whole ensemble of one

model is kept when at least one member yields a TG probability distribution between 1995 and 2014 that is similar to ERA5 *or* EOBS.

There are two reasons for this strategy:

1. As stated earlier, there is a small offset between TG in ERA5 and EOBS for the Paris area, which means that ERA5 would not pass the Kolmogorov-Smirnov test if EOBS was chosen as a reference (and vice versa). There is no reason to favor EOBS over ERA5, which does not include information in Paris *intra muros* (e.g., the Paris Montsouris station), and it is reasonable to compare CMIP6 with a climate model simulation that best resembles observations.
2. If a CMIP6 model yields an ensemble to sample internal variability, some of its members could be different from an observation reference during a 20-year period, because model years are not "real world" years. But we do not want to reject them, because if one member is satisfactory, it suggests that the model is able to reproduce observations over a 20-year period of time, so that scenario simulations could bring relevant information. Some models come with only one run, so that this test might exclude them if this only run does not pass a statistical test with observations. This encourages large ensemble approaches, as discussed by (Bevacqua et al., 2023).

This selection procedure obviously contains arbitrary elements (k-s test threshold, length of time series for comparisons, period of comparison, reference data, choice of variable for comparison).

As it is, this procedure selects 819 of the available 1288 simulations (with 585 SSP simulations), and 12 of the 26 CMIP6 models (outlined in boldface in Table 1).

2.3 Selection of events

An event exceeding 50°C is potentially very local and short lived, with an amplification by urbanization and surface water availability. We consider a small region that averages urban areas (Paris *intra-muros*) and suburban areas with forests. Due to the urban heat island effect, we estimate that 50°C can be exceeded within Paris, when TX exceeds 48°C over the Ile-de-France area. This assumption is justified by computing the differences of TX between observation at Paris Montsouris station, and the average over the Ile de France region (Figure 2). There is a systematic offset between TX in Paris-Montsouris and the average over the Paris area when TX exceeds 35°C. Therefore, we consider that TX exceeds 50°C in Paris when TX exceeds 48°C over Ile de France. This empirical threshold could be modified. We also verified that for extreme heat days, this temperature variation is typical of intra-region variations, over the last 10 years for which we could have access to more stations (from https://www.infoclimat.fr).

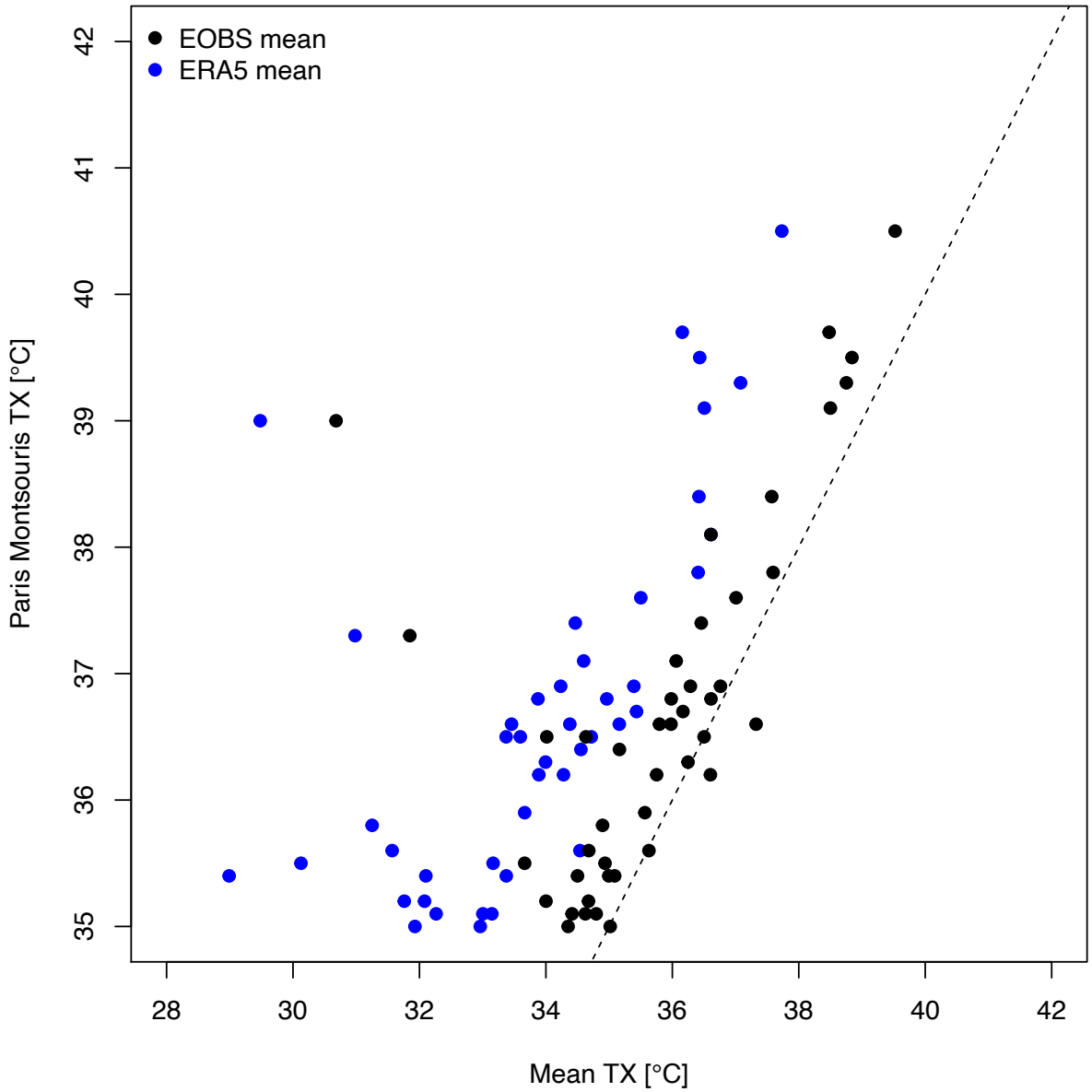

Figure 2: Scatter plot of TX in Paris Montsouris versus the average of TX over the region outlined in Figure 1, when TX exceeds 35°C in Paris Montsouris. The averages are computed from the EOBS (black circles) data and the ERA5 reanalysis (blue circles) data. The dashed line is the diagonal line.

From a list of 12 models and 585 simulations, we identified the years with at least one exceedance of 48°C before 2100. The results are summarized in Table 2 (not all model simulations in Table 1 reach 48°C before 2100).

Model name	Scenario	#members with TX>48°C/#Available members	First year with TX>48°C	GMST (°C)	GWI (°C)
CanESM5	ssp370	12/50	2079	18.6	3.5
CanESM5	ssp585	23/50	2071	19.2	3.9
CMCC-ESM2	**ssp245**	**1/1**	**2077**	**17.3**	**2.8**
CMCC-ESM2	ssp370	1/1	2071	17.3	2.8
CMCC-ESM2	**ssp585**	**1/1**	**2049**	**16.7**	**2.1**

ACCESS-CM2	ssp370	1/3	2099	18.8	4.1
EC-Earth3-AerChem	ssp370	1/1	2098	19.1	5.1
EC-Earth3-CC	ssp585	1/1	2093	19.6	4.9
EC-Earth3	ssp370	4/52	2094	18.6	3.4
EC-Earth3	ssp585	29/58	2080	18.5	3.5
EC-Earth3-Veg-LR	**ssp370**	**1/3**	**2058**	**16.3**	**2.7**
EC-Earth3-Veg-LR	ssp585	1/3	2094	19	5.4
EC-Earth3-Veg	ssp585	1/8	2091	18.9	4.6

Table 2: List of models with at least one simulation that exceeds 48°C in Paris at least for one day. We indicate the year of the first occurrence of TX>48°C among all members of the same scenario. The fifth column indicates the global surface temperature (GMST in °C) when the event occurs. The sixth column indicates the GMST difference (GWI, in °C) with a 1950-2000 baseline. The four simulations that are discussed in the results section are outlined in boldface.

3 Results

3.1 Event occurrence in CMIP6

We find that 8 models, among those selected to be realistic, exceed, at least once, 48°C between 2020 and 2100. Figure 3 and Table 2 report models for which at least one member in one scenario yields a TX>48°C event. Out of those 232 considered CMIP6 simulations, 81 simulations yield at least one TX>48°C event.

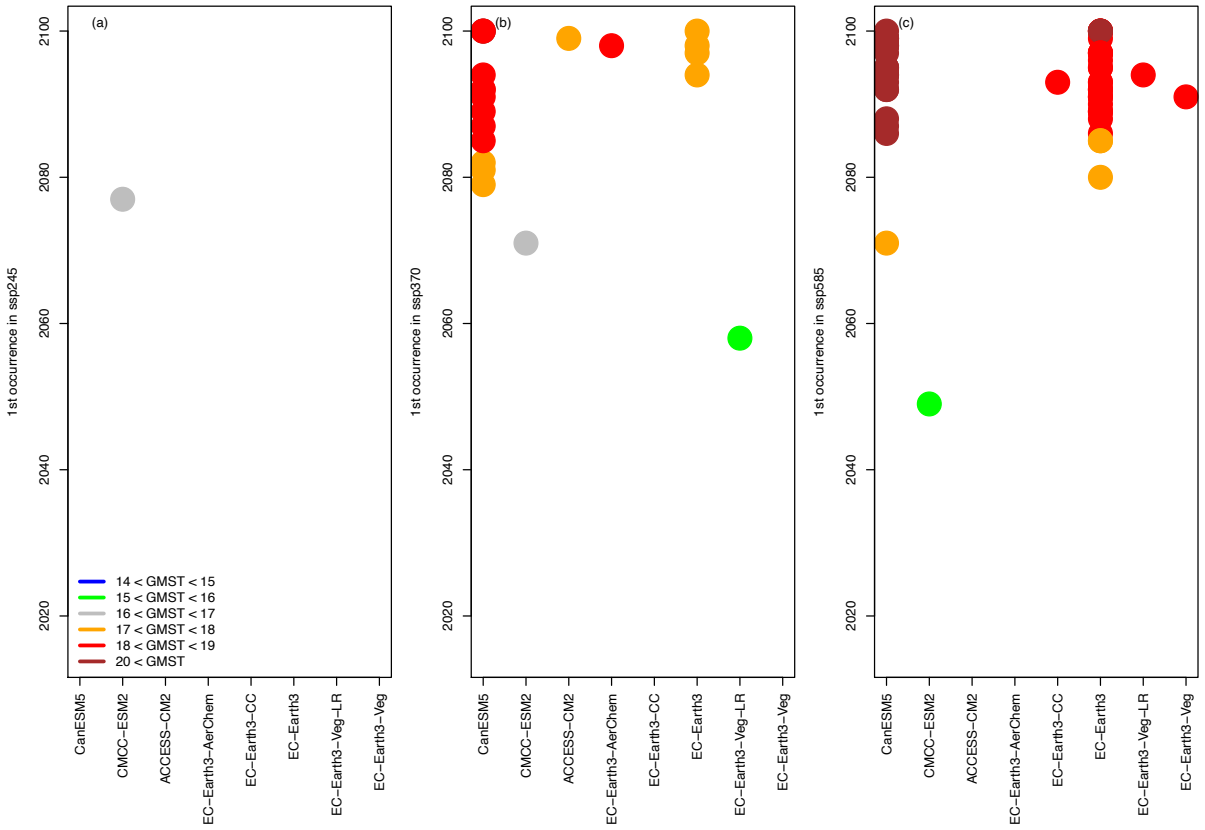

Figure 3: Time of first exceedance of 48°C in CMIP6 models for four SSP scenarios. The vertical axis indicates the year of first occurrence of TX>48°C in the Ile-de-France region, including Paris in model simulations. TX can exceed 48°C at later years, but this is not reported in the figure. The colors indicate the GMST for the 20 years around the year of TX>48°C (panel (a) for legend).

We first consider the four SSP separately. For illustration purposes, we select the model simulations with the earlier dates that reach 48°C in the Paris area. We find that TX never exceeds 48°C in the SSP1-2.6 scenario. Therefore, we focus on SSP2-4.5, SSP3-7.0 and SSP5-8.5 (Figure 3). Only CMCC-ESM2 reaches the threshold with SSP2-4.5 (Figure 3a). This model was run with only one member.

We computed the GMST increase (GWI) of the decades around each event since a 1950-2000 baselines. From Figure 4, it appears that TX>48°C events in CMIP6 simulations occur when the GWI exceeds 2°C.

Most of the selected CMIP6 simulations (with 2 exceptions) do not reach this threshold as long as the GMST does not exceed 16°C (Figure 3), which correspond to a GWI of about 2.5°C since 1950-2000 (Figure 4). As reaching this temperature is physically possible (Noyelle et al., 2023; Zhang and Boos, 2023), those simulations will be discussed in this paper.

There is a shift of CMIP6 model behavior with SSP3-7.0, where 6 models reach the 48°C threshold between 2079 and 2100 (i.e., within the expected lifetime of the junior authors of this paper). The GWI for those models is larger than 2.7°C (with respect to a 1950-2000 baseline: Figure 4).

With SSP5-8.5, eight models reach the 48°C threshold between 2049 and 2100, with GWI warming larger than 2.1°C (with respect to a 1950-2000 baseline). Two models (CMCC-ESM5 and EC-Earth-Veg-LR) reach this threshold before 2055 (i.e., within the expected lifetime of the senior authors of this paper).

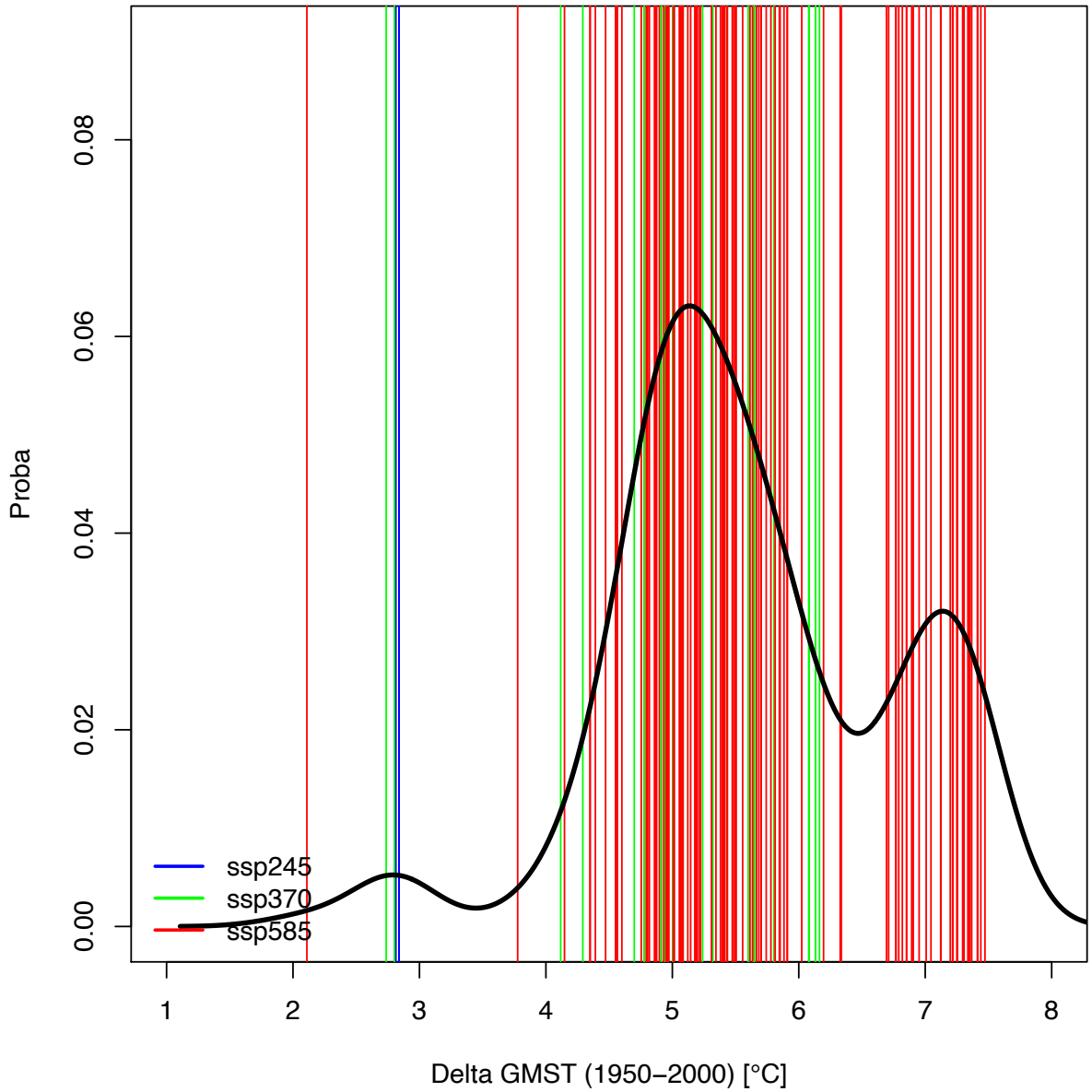

Figure 4: Distributions of GMST increase (GWI) values when TX>48°C in Paris, from reference baselines of GMST in 1950-2000. The vertical bars indicate all occurrences of TX>48°C. The colors indicate the SSP scenario of the TX>48°C event occurrences. The black line is an empirical probability density function of the year of occurrence of TX>48°C.

We pooled all 81 simulations for which TX exceeds 48°C and estimated an empirical probability function for GWI values from a 1950-2000 baseline. The empirical probability was weighted by the total number of considered simulations (232). This gives a crude idea of the probability to exceed the 48°C threshold for GWI levels of warming. There are more sophisticated ways of obtaining such probabilities, in particular using Extreme Value Theory (Coles, 2001; Robin and Ribes, 2020). We defer such analyses to a future paper.

We notice that a peak probability is obtained when GWI (from 1950-2000) is around 5°C (around 6% chance). If GWI is lower than 2°C, this probability is negligible. It becomes measurable (1% chance) when GWI reaches ~2.7°C.

3.2 Daily summer variations for heat events

We select the first occurrence of TX>48°C for each SSP scenario. We hence retain CMCC-ESM2 for SSP2-4.5, EC-Earth3-Veg-LR for SSP3-7.0 and CMCC-ESM2 for SSP5-8.5 (Table 2). This choice is obviously arbitrary from the physical point of view. For illustration purposes, we will

focus on the earliest occurrences, i.e., the events that the authors of this paper are likely to witness.

The summer time series of daily TX and TM (from June 1st to August 31st) are shown in Figure 5 for the four selected model, along with the already experienced extremes of 2003 and 2022. Apart from the T>48°C peaks, the distributions of temperatures are within the variations observed during the hot summers of 2003 and 2022, which shows that the whole summers are already warm. Météo-France defines a heatwave ("canicule") in Paris when TX exceeds 31°C and TN exceeds 21°C [REF]. Such a definition depends on the region, with higher thresholds in the Southern part of France. Due to the urban effects that were identified before, we can lower such a threshold to 29°C for TX, as rough estimates over the Paris region. We retain a 20°C threshold for TN, as it defines tropical nights.

We find that reaching a 48°C peak is obtained during warm summers (according to present-day standards: Figure 5), with a large number of days above the mean seasonal cycle. During those summers the values of TX exceed 29°C and TN exceed 20°C on several occasions, which means that several heatwaves (similar to those of 2003 and 2022) also occur during the course of those summers. The peaks of TX>48°C correspond to TX anomalies of more than 20°C above the present-day seasonal cycle and last for one day.

The selected simulations show periods of tropical nights (i.e., when the minimal daily temperature TN exceeds 20°C). We note that the warmest tropical nights do not necessarily occur on the same day as the warmest TX, although tropical nights do occur when TX is high.

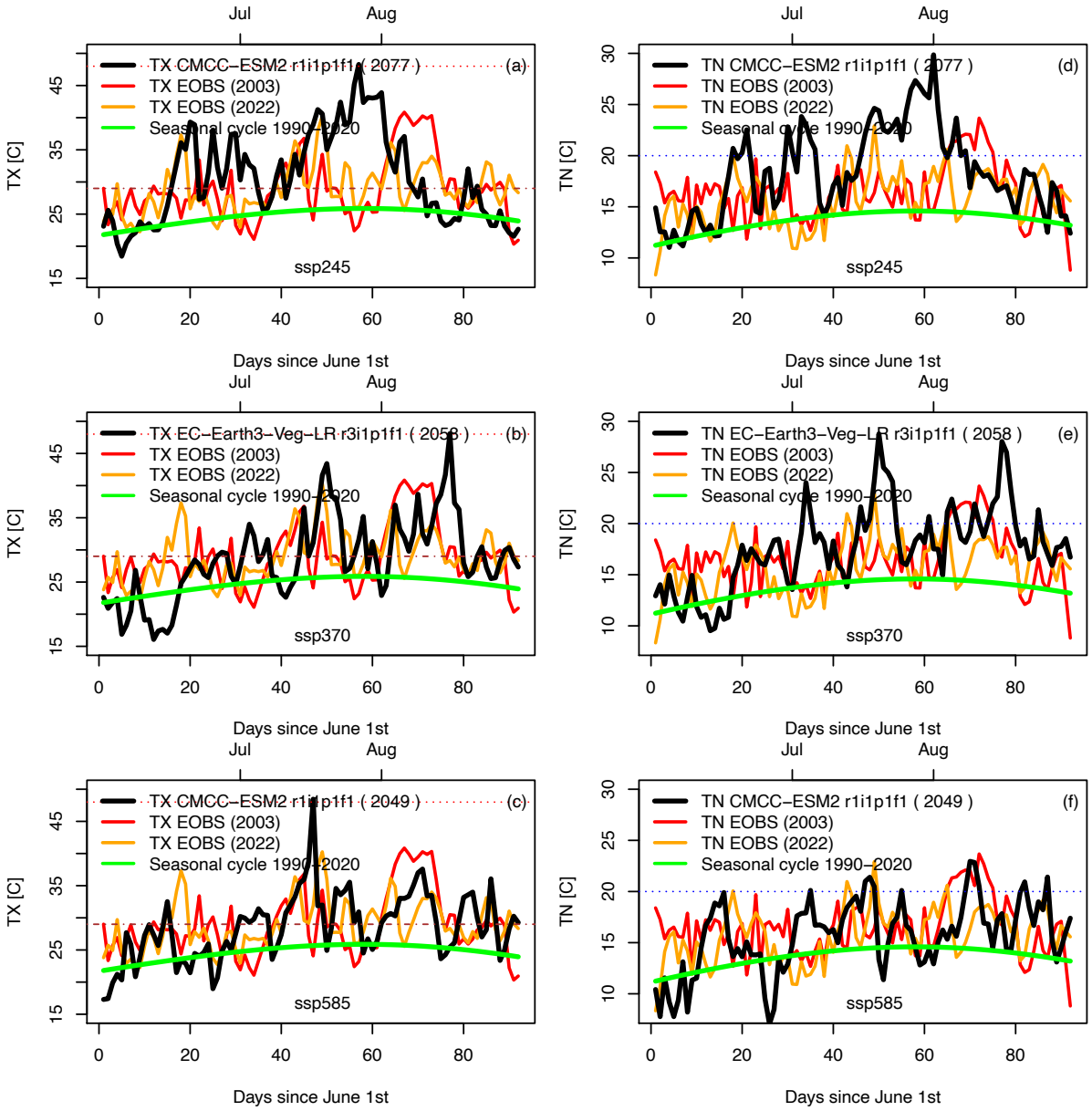

Figure 5: Time series of daily maximum (TX: left column) and minimum (TN: right column) temperatures in the Paris area for three scenarios. Black lines indicate TX and TN in models. Red and orange lines indicate TX and TN in EOBS for the summers of 2003 and 2022 (respectively). The horizontal red dotted line indicates the 48°C threshold for TX. The horizontal dashed brown lines indicate the 29°C TX threshold for heatwaves. The horizontal blue dotted line indicates 20°C (TN threshold for tropical nights). The green lines indicate the seasonal cycle for TX and TN, computed from the EOBS data (1990-2020).

3.3 TX and SLP patterns

The temperature patterns over France and the atmospheric circulation patterns over the Eastern North Atlantic during the four events are shown in Figure 6 to Figure 8.

For SSP2-4.5, we selected the CMCC-ESM5 model. The TX>48°C event occurs in July 2077, with a GWI of ~2.3°C. The maximum TX anomaly is near the Paris region and TX exceeds 40°C over most of France (Figure 6a). Therefore, the heat event over Paris is also obtained for many gridcells of the model around the Paris region. The atmospheric circulation pattern shows an anticyclone over Scandinavia, and lows over France and west of France (Figure 6b). This atmospheric pattern also corresponds to observed heatwaves of 2003 and 2022 in France [REF].

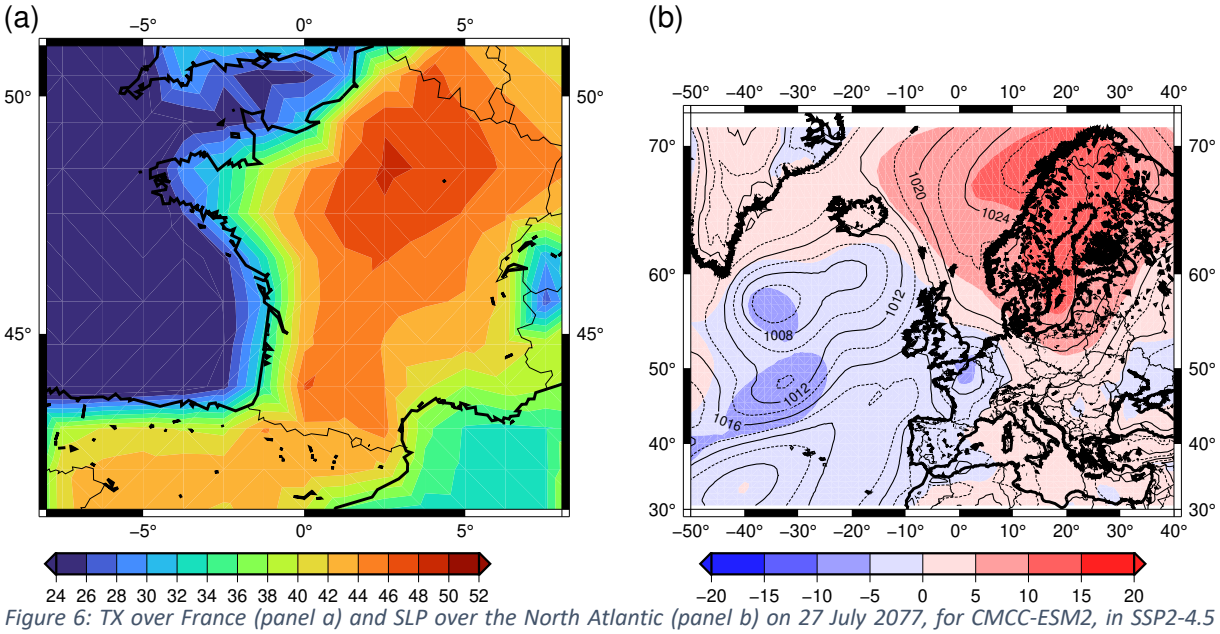

Figure 6: TX over France (panel a) and SLP over the North Atlantic (panel b) on 27 July 2077, for CMCC-ESM2, in SSP2-4.5 (r1i1p1f1). TX (panel a) is expressed in °C. SLP is expressed in hPa (isolines in panel b). Colors in panel (b) correspond to anomalies of SLP (in hPa) with respect to the summer average.

For SSP3-7.0, we selected the EC-Earth3-Veg-LR model. TX exceeds 48°C on the 16th of August 2077 in the r3i1p1f1 member, i.e. after the apex of the seasonal cycle. The GWI from 1950-2000 is ~2.7°C. The center of the extreme anomaly is located in North East France (Figure 7a). The hot anomaly covers most of France, with TX values above 40°C over most of the country. The atmospheric circulation shows an anticyclonic pattern between Iceland and Scandinavia and in Central Europe. The circulation yields a strong cyclonic pattern west of Ireland (Figure 7b). Such a pattern is likely to convey warm air from North Africa into France.

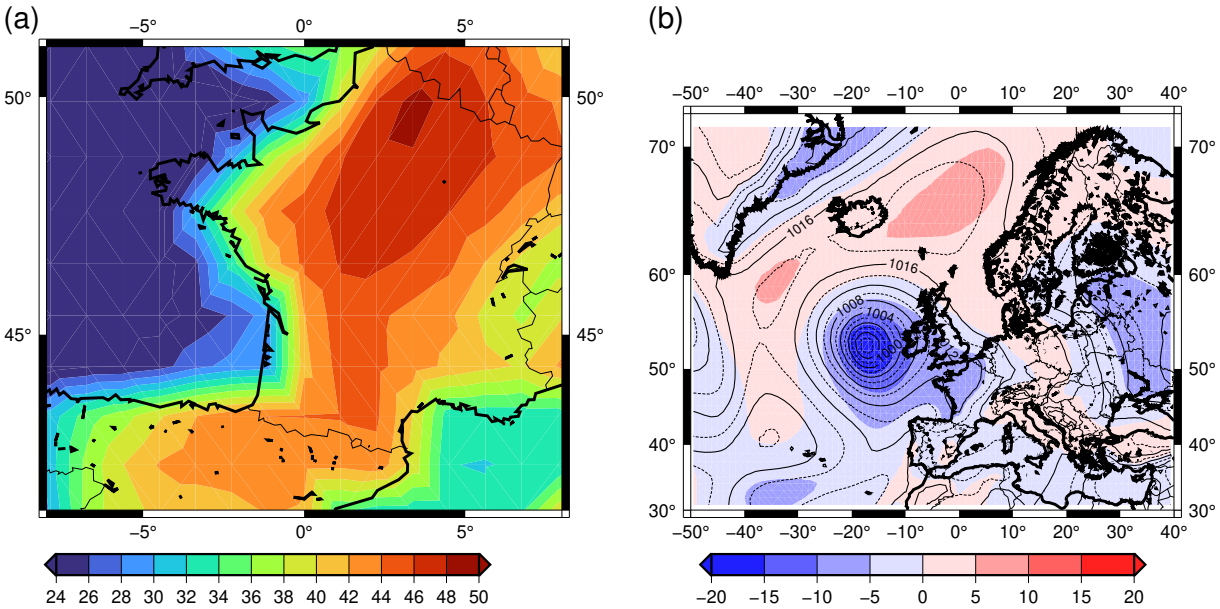

Figure 7: TX over France (panel a) and SLP over the North Atlantic (panel b) on 16 August 2058, for EC-Earth3-Veg-LR, in SSP3-7.0 (r3i1p1f1). TX (panel a) is expressed in °C. SLP is expressed in hPa (isolines in panel b). Colors in panel (b) correspond to anomalies of SLP (in hPa) with respect to the summer average.

For SSP5.8-5, the early TX>48°C event occurs in July 2049 in CMCC-ESM2 with a GWI of ~2.1°C (since 1950-2000). The center of the event occurs in the South West of France, with

temperatures exceeding 50°C (Figure 8a). Most of the country yield TX over 42°C. Northern Spain is also affected by high temperatures. The heat does not extend to the east of France. The atmospheric circulation pattern yields an anticyclonic feature east of France (centered over the Balkans), and a depression between Iceland and Brittany (Figure 8b). In both cases, the presence of a depression on the west side of the heatwave likely increases temperature over France via southerly advection or diabatic heating in the frontal area.

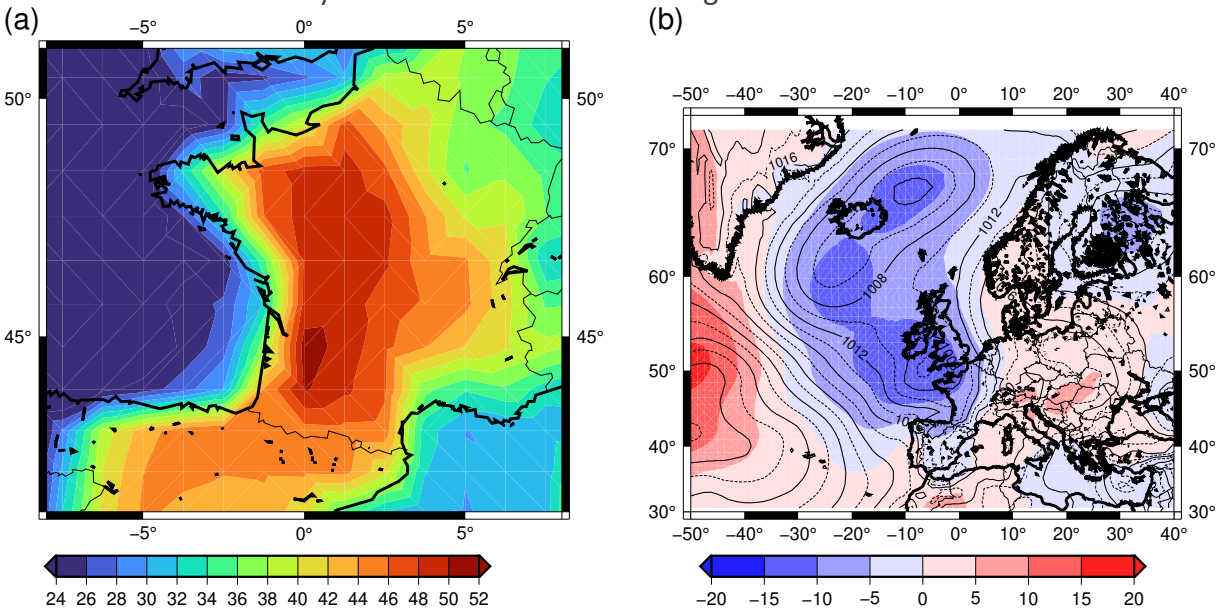

Figure 8: TX over France (panel a) and SLP over the North Atlantic (panel b) on 07 July 2049, for CMCC-ESM2, in SSP5-8.5 (r1i1p1f1). TX (panel a) is expressed in °C. SLP is expressed in hPa (isolines in panel b). Colors in panel (b) correspond to anomalies of SLP (in hPa) with respect to the summer average.

Out of those three events (from three SSP scenarios, and three different climate models), three events occur with a GWI between 2.1°C and 2.8°C. Those three events yield atmospheric patterns that are reminiscent of already observed heatwaves in Paris, albeit with exacerbated TX values.

4 Discussion

This paper presents a simple approach to outline extreme temperature events in a large urban and sub-urban region surrounding (and including) Paris. The methodology is based on data inspection and does not contain any sophisticated statistical (Parey, 2008; Yiou and Jézéquel, 2020) or physical (Ragone et al., 2018; Gessner et al., 2021) modelling approaches. Those results serve as a first step for further in-depth studies of extreme heatwaves.

Many choices have been subjective (or based on previous experience): threshold of temperature daily increments, global covariate, and general frequency of extremes. The results were obtained on the IPSL computing facility, for which a (large) subset of the simulations of CMIP6 are available. The same computations are possible with access to Earth System Grid Federation (ESGF) servers throughout the world, although they would require downloading a large amount of data.

We have not discussed in detail the mechanisms leading to hot extremes in Paris, which is left for further studies. There are fairly substantial differences in the large-scale circulation patterns occurring those events.

5 Practical implications

We have identified events corresponding to moderate GMST increase (between 2.1 and 2.8°C). Those events come with spates of tropical nights (minimum temperatures over 20°C), which would exacerbate the impacts on health of exceeding 50°C during the day. Some of the Paris events correspond to larger scale events, where temperature exceeds 50°C (e.g., in the south west of France) and large parts of the country have TX above 40°C. Therefore, a crisis in Paris would also be reflected in other regions of France, where temperatures could even be higher, especially in urban areas (in Amiens: Figure 7a; or in Bordeaux: Figure 8a).

We have not quantified the probability of exceeding this high threshold, because it is rarely observed more than once in each simulation. This probability is deemed to be negligible for a global surface temperature increase lower than 2°C within the next two decades. It increases to ~1% chance if the global surface temperature increases by 2.7°C. Yet, it cannot be excluded, because Western Europe warms faster than the rest of the world [REF], and temperature has already reached 48.8°C in Sicily (Southern Italy) in August 2023. If global surface temperature (GMST) increases by more than 4°C since 1950-2000, the probability of such hot events increases dramatically in the CMIP6 database.

6 Conclusion

This paper aims at exploring how a temperature of 50°C could be reached in the Paris area, by examining the CMIP6 database. The general questions where: when? what level of global warming? What type of meteorology? Exploring the CMIP6 database poses a few statistical, physical and computing challenges that are tackled in the paper.

This paper is meant to provide a data-processing chain for the analysis of extremes in this simulation ensemble, with an illustration for the Paris area. This serves as a demonstrator for a climate service for policymakers, which can be transposed to other regions in the world.

We do not propose a complete climate analysis of the events (which would be an entire paper by itself) and focused on extremely simple diagnostics. Hence this data-processing chain can serve as a preliminary step to identify relevant (in the sense that was defined in the methods section) simulations, and avoid sophisticated (and computer costly) steps of bias correction.

7 Acknowledgements

This paper was motivated by the Groupe régional d'expertise sur le changement climatique et la transition écologique (GREC) in Île-de-France. We thank the ESPRI computing mesocenter at IPSL for making the CMIP6 data available.

8 Funding sources

This paper received the support of the grant ANR-20-CE01-0008-01 (SAMPRACE). This work also received support from the European Union's Horizon 2020 research and innovation programme under grant agreement No. 101003469 (XAIDA). PY also acknowledges the support from ANDRA and EDF (grant COSTO).

9 Code and data availability

The codes (in R, cdo and shell scripts) to perform all data processing computations is available from https://github.com/pascalyiou/Paris50C.git

The CMIP6 data files are available from the IPSL ESGF node: https://esgf-node.ipsl.upmc.fr/projects/esgf-ipsl/

ERA5 reanalysis and E-OBS data sets were retrieved from the Climate Explorer: https://climexp.knmi.nl/ . We extracted tasmax and tasmin over the region outlined in Figure 1, directly from the Climate Explorer.

10 Declaration of generative AI in writing

This manuscript was entirely written by its authors, without any use of generative AI.

11 Author contribution

RV and NdN initiated the study. PY drafted the manuscript and ran the computations. YR provided Figure 1. RN and FdA provided input on the analyses of the manuscript. All authors contributed to the writing of the manuscript.

12 References

Arnold, B. C., Balakrishnan, N., and Nagaraja, H. N.: Records, John Wiley & Sons, 2011.

Bador, M., Terray, L., Boe, J., Somot, S., Alias, A., Gibelin, A.-L., and Dubuisson, B.: Future summer mega-heatwave and record-breaking temperatures in a warmer France climate, Environmental Research Letters, 12, 074025, 2017.

Bastos, A., Fu, Z., Ciais, P., Friedlingstein, P., Sitch, S., Pongratz, J., Weber, U., Reichstein, M., Anthoni, P., and Arneth, A.: Impacts of extreme summers on European ecosystems: a comparative analysis of 2003, 2010 and 2018, Philosophical Transactions of the Royal Society B, 375, 20190507, 2020.

Bevacqua, E., Suarez-Gutierrez, L., Jézéquel, A., Lehner, F., Vrac, M., Yiou, P., and Zscheischler, J.: Advancing research on compound weather and climate events via large ensemble model simulations, Nature Communications, 14, 2145, 2023.

Carvalho, D., Pereira, S. C., and Rocha, A.: Future surface temperatures over Europe according to CMIP6 climate projections: an analysis with original and bias-corrected data, Climatic Change, 167, 1–17, 2021.

Coles, S.: An introduction to statistical modeling of extreme values, Springer, London, New York, 208 pp., 2001.

Deser, C., Terray, L., and Phillips, A. S.: Forced and internal components of winter air temperature trends over North America during the past 50 years: Mechanisms and implications, Journal of Climate, 29, 2237–2258, 2016.

Domeisen, D. I., Eltahir, E. A., Fischer, E. M., Knutti, R., Perkins-Kirkpatrick, S. E., Schär, C., Seneviratne, S. I., Weisheimer, A., and Wernli, H.: Prediction and projection of heatwaves, Nature Reviews Earth & Environment, 4, 36–50, 2023.

Eyring, V., Bony, S., Meehl, G. A., Senior, C. A., Stevens, B., Stouffer, R. J., and Taylor, K. E.: Overview of the Coupled Model Intercomparison Project Phase 6 (CMIP6) experimental design and organization, Geoscientific Model Development, 9, 1937–1958, 2016.

Fischer, E. M., Sippel, S., and Knutti, R.: Increasing probability of record-shattering climate extremes, Nature Climate Change, 11, 689–695, 2021.

Fischer, E. M., Beyerle, U., Bloin-Wibe, L., Gessner, C., Humphrey, V., Lehner, F., Pendergrass, A. G., Sippel, S., Zeder, J., and Knutti, R.: Storylines for unprecedented heatwaves based on ensemble boosting, Nature Communications, 14, 4643, 2023.

Florentin, A. and Lelievre, M.: Mission d'information et d'évaluation du Conseil de Paris Paris à 50 degrés : s'adapter aux vagues de chaleur, Paris City Council, 2023.

Gessner, C., Fischer, E. M., Beyerle, U., and Knutti, R.: Very rare heat extremes: quantifying and understanding using ensemble re-initialization, Journal of Climate, 1–46, 2021.

Haylock, M. R., Hofstra, N., Tank, A. M. G. K., Klok, E. J., Jones, P. D., and New, M.: A European daily high-resolution gridded data set of surface temperature and precipitation for

1950-2006, J. Geophys. Res. - Atmospheres, 113, doi:10.1029/2008JD010201, 2008.
Hersbach, H., Bell, B., Berrisford, P., Hirahara, S., Horányi, A., Muñoz-Sabater, J., Nicolas, J., Peubey, C., Radu, R., and Schepers, D.: The ERA5 global reanalysis, Quat. J. Roy. Met. Soc., 146, 1999–2049, 2020.
Maraun, D. and Widmann, M.: Statistical downscaling and bias correction for climate research, Cambridge University Press, 2018.
National Academies of Sciences Engineering and Medicine (Ed.): Attribution of Extreme Weather Events in the Context of Climate Change, The National Academies Press, Washington, DC, https://doi.org/10.17226/21852, 2016.
Noyelle, R., Zhang, Y., Yiou, P., and Faranda, D.: Maximal reachable temperatures for Western Europe in current climate, Environ. Res. Lett., 18, 094061, https://doi.org/10.1088/1748-9326/acf679, 2023.
Parey, S.: Extremely high temperatures in France at the end of the century, Climate Dynamics, 30, 99–112, https://doi.org/DOI 10.1007/s00382-007-0275-4, 2008.
Philip, S. Y., Kew, S. F., van Oldenborgh, G. J., Anslow, F. S., Seneviratne, S. I., Vautard, R., Coumou, D., Ebi, K. L., Arrighi, J., Singh, R., van Aalst, M., Pereira Marghidan, C., Wehner, M., Yang, W., Li, S., Schumacher, D. L., Hauser, M., Bonnet, R., Luu, L. N., Lehner, F., Gillett, N., Tradowsky, J. S., Vecchi, G. A., Rodell, C., Stull, R. B., Howard, R., and Otto, F. E. L.: Rapid attribution analysis of the extraordinary heat wave on the Pacific coast of the US and Canada in June 2021, Earth Syst. Dynam., 13, 1689–1713, https://doi.org/10.5194/esd-13-1689-2022, 2022.
Quintana-Segui, P., Le Moigne, P., Durand, Y., Martin, E., Habets, F., Baillon, M., Canellas, C., Franchisteguy, L., and Morel, S.: Analysis of near-surface atmospheric variables: Validation of the SAFRAN analysis over France, Journal of applied meteorology and climatology, 47, 92–107, 2008.
Ragone, F., Wouters, J., and Bouchet, F.: Computation of extreme heat waves in climate models using a large deviation algorithm, Proc. Nat. Acad. Sci., 115, 24–29, 2018.
Riahi, K., Van Vuuren, D. P., Kriegler, E., Edmonds, J., O'neill, B. C., Fujimori, S., Bauer, N., Calvin, K., Dellink, R., and Fricko, O.: The Shared Socioeconomic Pathways and their energy, land use, and greenhouse gas emissions implications: An overview, Global environmental change, 42, 153–168, 2017.
Robin, Y. and Ribes, A.: Nonstationary extreme value analysis for event attribution combining climate models and observations, Advances in Statistical Climatology, Meteorology and Oceanography, 6, 205–221, 2020.
von Storch, H. and Zwiers, F. W.: Statistical Analysis in Climate Research, Cambridge University Press, Cambridge, 2001.
Yin, J., Gentine, P., Slater, L., Gu, L., Pokhrel, Y., Hanasaki, N., Guo, S., Xiong, L., and Schlenker, W.: Future socio-ecosystem productivity threatened by compound drought–heatwave events, Nature Sustainability, 6, 259–272, 2023.
Yiou, P. and Jézéquel, A.: Simulation of extreme heat waves with empirical importance sampling, Geosci. Model Dev., 13, 763–781, https://doi.org/10.5194/gmd-13-763-2020, 2020.
Zhang, Y. and Boos, W. R.: An upper bound for extreme temperatures over midlatitude land, Proceedings of the National Academy of Sciences, 120, e2215278120, 2023.